Eur. Phys. J. D **28**, 193–198 (2004)
DOI: 10.1140/epjd/e2003-00302-7

THE EUROPEAN PHYSICAL JOURNAL D

Laser-induced control of (multichannel) intracluster reactions

The slowest is always the easiest to take

A. González Ureña[1,a], K. Gasmi[1], S. Skowronek[1], A. Rubio[2], and P.M. Echenique[2]

[1] Unidad de Láseres y Haces Moleculares, Instituto Pluridisciplinar, Universidad Complutense de Madrid, Juan XXIII-1°, 28040 Madrid, Spain
[2] Dpto. Fisica de Materiales, Facultad de Químicas, Universidad del País, Vasco/Euskal Herriko Unibertsitatea, Centro Mixto CSIC-UPV/EHU and Donostia International Physics Center (DIPC), Apdo. 1072, 20018 San Sebastián/Donostia, Spain

Received 3 July 2003
Published online 2nd December 2003 –

Abstract. An experimental and theoretical study on the excited $Ba\cdots FCH_3(A)$ photodissociation yield as a function of the excitation laser fluence is reported. Experimentally, it was found that the two-photodissociation channel yields, i.e. the reactive BaF and non-reactive Ba^* products, increased exhibiting a similar behaviour, as the laser fluence changed from 0.2 up to ca. 4 mJ/cm^2. Beyond this value the BaF yield levels off and the Ba^* decreases over the 4–7 mJ/cm^2 range. The theoretical simulation of the excited state electron-ion dynamics within the time-dependent density functional theory revealed that the reactive channel dominated the photofragmentation dynamics as it occurs within a femtosecond time scale and became accelerated as the photodissociation laser fluence increased. By contrast, the non-reactive channel only manifested for low laser fluences at the nano/picosecond time regime resulted inactive as the laser fluence increased. A simple scheme to control the dynamics of the intracluster multichannel reaction is suggested in which *the slowest the channel the easiest to close it* as the excitation laser power increases.

PACS. 36.40.Jn Reactivity of clusters – 36.40.Qv Stability and fragmentation of clusters – 34.50.Rk Laser-modified scattering and reactions

Laser control of chemical reactions is currently attracting a considerable attention from both theoretical and experimental point of view [1–3]. Among several schemes to implement such an objective one of the most promising is based on quantum interference. For unimolecular reactions, in which a single reactant molecule is transformed to several product molecules, two types of control have been applied insofar. Namely, the "two-beam interference" [4–6] and the "two-pulse time delay" control [7,8]. While these two control schemes are based on a limited number of optimisation parameters (i.e., the phase difference between the two lasers and the time delay between the pump and dump laser pulses, respectively) a new powerful method has been developed [9] based on the adaptative shaping of femtosecond laser pulses which works satisfactorily even for complex systems. Although, in many cases, the electron/ion dynamics of the system is not fully understood, there are examples in which the dynamics of a unimolecular reaction induced by an optimal femtosecond pulse, generated from adaptative learning algorithms, has been deciphered [10].

In this work, we report on the control of the $Ba\cdots FCH_3 + h\nu \rightarrow BaF + CH_3$ intracluster reaction achieved by changing the fluence of the excitation laser. The spectroscopy and photofragmentation dynamics of the $Ba\cdots FCH_3$ weakly bound complex have been studied using both nanosecond [11,12] and femtosecond laser techniques [13,14]. Thus, when this cluster is excited to its A state two photofragmentation channels are opened. The reactive one leading into BaF and FCH_3. products and the non-reactive one producing Ba^* and FCH_3. Furthermore, it is shown how these two photofragmentation channel yields exhibited distinct behaviour particularly at high laser fluences. In other words, the product $[Ba^*]/[BaF]$ branching ratio changes and tends to zero going from low to high laser fluence conditions. The present work extends the preliminary results reported in reference [15] using different laser for the excitation step confirming the suggested multichannel control of the $Ba\cdots FCH_3$ photofragmentation. The experimental study is complemented with extensive theoretical excited-state electron-ion simulations based on the time-dependent density functional theory (TDDFT) [16,17] methodology. Indeed,

[a] e-mail: laseres@pluri.ucm.es

the calculations of the excited state electron-ion dynamics provided a clear picture of the cluster photodissociation dynamics revealing a distinct time evolution associated with each individual reaction channel. We anticipate that the different two-channel time dynamics as the laser intensity of the excitation step is changed, is the factor that makes possible the control of the multichannel laser-induced reaction.

A detailed description of the molecular beam apparatus is given elsewhere [12], briefly, the weakly bound complex $BaF\cdots CH_3$ is produced in a laser vaporisation source followed by supersonic expansion, using a gas mixture of He with a 10% of FCH_3. The molecular beam is then probed inside a different chamber using a laser ionisation coupled with a linear time-of-flight mass spectrometer. Two lasers are used for the probing of the molecular beam: a tunable laser induces the reaction in the $Ba\cdots FCH_3$ weakly bound complex, while a second laser ionises the complex and the photofragmentation products: a dye laser with a bandwidth of typical 0.1 cm^{-1} and a pulse duration of 8 ns is used for excitation of the complex, while the fourth harmonic of a continuum NY80 Nd-YAG laser (266 nm, pulse duration 7 ns) is used for ionisation. The excitation laser arrives about 8–10 ns earlier to the beam-laser interaction region than the ionisation laser [18]. A key feature of the experimental technique is the simultaneous measurement of both the complex photodepletion and the product action spectra (see Ref. [19] for further details). We measured simultaneously the $Ba\cdots FCH_3^+$, BaF^+ and Ba^+ signal at two different conditions: (a) using UV photons ($\lambda = 266$ nm) only and (b) using first a pump dye laser ($\lambda = 617.7$ nm) and then, 10 ns later, the UV laser ($\lambda = 266$ nm). The BaF and Ba action signals were estimated from their (b)–(a) signal, respectively. This procedure was then repeated at different excitation laser fluences. The latter was modified by using a high-energy variable attenuator (Newport mod. 935-5-OPT). This procedure ensured that the focus and optical features of the laser beam remained unchanged.

The pump and probe scheme used in the present experiment is the following. First, $Ba\cdots FCH_3 + h\nu_{pump}$ ($\lambda = 617.7$ nm) $\rightarrow BaF + CH_3$ or $Ba^* + FCH_3$, then the probe laser $h\nu_{probe}$ ($\lambda = 266$ nm) is used to ionised the BaF and Ba^* species and measure their population. The BaF^+ signal is produced by direct one photon ionisation of BaF product absorption of the 266 nm photon, as demonstrated in a previous work (see for example Fig. 2 of Ref. [19]). With respect to the Ba^* product direct one photon ionisation of Ba ground state is not possible at 266 nm, so only metastable Ba^* product can be ionized (see Fig. 2 of Ref. [20] for an energy diagram of the system here investigated). Under the present experimental conditions, the 266 nm probing laser intensity was always kept at a very low intensity to guarantee that a two photon absorption process was, if any, a very minor effect [15]. It should be recalled that the pumping laser wavelength excites the A $\leftarrow$ X electronic transition of the $Ba\cdots FCH_3$ complex only, i.e. it does not affect the free Ba atoms present in the beam expansion at all (see Ref. [12] for details).

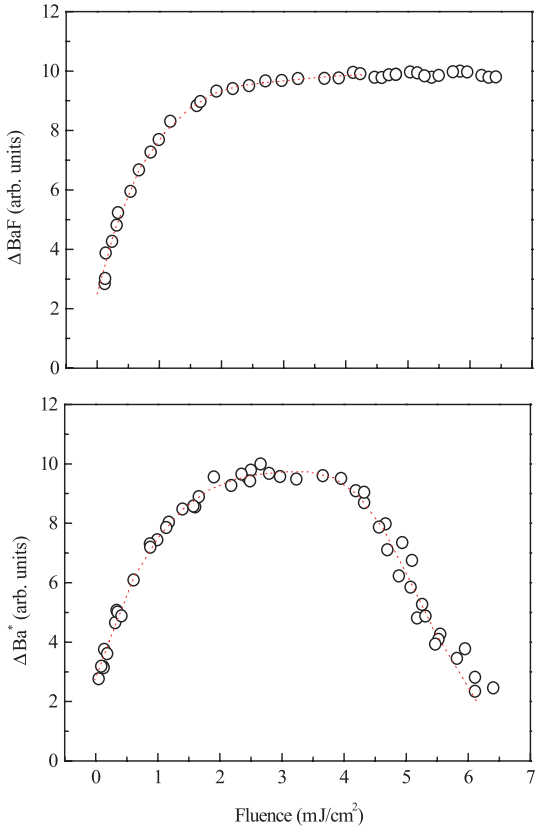

Fig. 1. $Ba\cdots FCH_3$ photofragmentation channel yields as a function of the laser fluence: (top) ΔBaF signal obtained by the procedure described in the text, (bottom) ΔBa^* signal. Dotted lines are just a guide to the eye.

The measured Ba^* and BaF photofragmentation channel yields are displayed in Figure 1 as a function of the laser fluence. Both ΔBa^* and ΔBaF signals were obtained using the same procedure. The ΔBa^* was calculated by subtracting the Ba^* (UV) signal from the Ba^* (UV + VIS) signal. Here UV and VIS stand for the signal measured when the ultraviolet probe laser and a dye pump laser, respectively. The same procedure was followed to obtain ΔBaF. The most interesting feature is the laser fluence dependence of both reactive, ΔBaF, and non-reactive, ΔBa^*, yields. While ΔBa^* increases reaching a maximum around 4 mJ/cm^2 with a subsequent decline beyond this fluence value, the ΔBaF increases over the small laser fluence range and subsequently levels off. Clearly, the $[Ba^*]/[BaF]$ branching ratio, as depicted in Figure 2, depends on the laser field employed to induce the reaction and, more specifically, it diminishes with the laser fluence beyond ca. 4 mJ/cm^2.

In order to understand the physical mechanism underlying the electron/ion dynamics of this $Ba\cdots FCH_3$ complex, we performed extensive excite state simulations within a TDDFT formalism as implemented by some of us in the octopus code [21]. In general, TDDFT has been very successful in describing the optical spectra of small

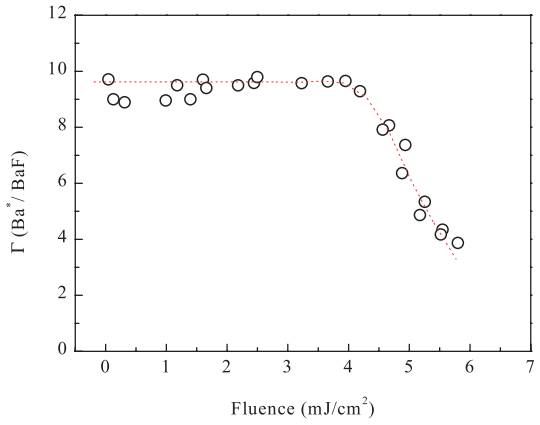

Fig. 2. Laser fluence dependence of the [Ba*]/[BaF] branching ratio. Points: present experimental results; dotted line is just a guide through the points.

nanostructured materials [16,17], including high-intense laser-induced electronic-ion dynamics [22]. All dynamical quantities are computed by evolving the electronic wave functions in real-time and real-space [23] and treating the electron-ion interaction by norm-conserving pseudopotentials [24]. The set of equations to be solved for the combined electron-ion dynamics are the time-dependent Kohn-Sham equation (in atomic units): $-id\psi_i(r,t)/dt = [H_0(n(r,t)) + V_{\rm laser}(r,t)]\psi_i(r,t)$ and the Newton's equation for the nuclei motion: $M_\alpha d^2R_\alpha(t)/dt^2 = F_\alpha(R,t)$. Here $V_{\rm laser}(r,t)$ describes the classical time-dependent external electromagnetic field acting on our system, ψ_i are the occupied Kohn-Sham orbitals, and H_0 is the standard Kohn-Sham Hamiltonian that includes the (pseudo)ion-potential, the repulsive electronic Hartree potential, and the exchange-correlation potential that in the present work it is described in the local-density approximation (LDA) [25] that now are time-dependent functions through the time dependence of the density ($n(r,t) = \Sigma_i^{occ}|\psi_i(r,t)|^2$). Finally, in the Newton equation for the nuclei (R_α, M_α) stands for the coordinate of the nucleus and its mass. The force F_α exerted on it is calculated through Ehrenfest's theorem [21]. As for technical details, we confined the molecule within a sphere of radii 12 Å. The space is discretised using a uniform grid spacing of 0.16 Å and for the time evolution we used a time-step of 0.0016 fs. Those parameters ensure the stability of the time-dependent propagation and yield spectra with a resolution better than 0.1 eV.

The initial configuration for the laser induced reactivity is the ground state of the weakly bound Ba$\cdots$FCH$_3$ complex. We have relaxed the molecular structure and obtained a rather good agreement with previous CI calculations [26] for bond lengths (differences of 2%) as well as ionisation potential (the calculated value is 4.9 eV to be compared with the CI value of 4.55 eV [26] and the measured one of (4.5 ± 0.1) eV [11]). The present approach was first tested by computing the optical absorption cross-section of Ba$\cdots$FCH$_3$. The calculated and experimental spectrum is in excellent agreement (see Fig. 3). It is interesting to note that the main peak corresponds to a HOMO-LUMO like transition with major weight on the Ba atom. However, this $6s \rightarrow 6p$ atomic-like transition of the Ba atom has been redshifted with respect to the calculated isolated Ba absorption peak at about 2.4 eV. This renormalization of the atomic transition stems from a polarization of the atomic cloud around the Ba atom due to the dipole of the FCH$_3$ part (this is clearly seen in the shape of the HOMO-LUMO orbitals in Fig. 3). Also it is important to note that the Kohn-Sham difference of HOMO-LUMO eigenvalues is 1.6 eV showing the error of using the one-electron eigenvalues as fingerprints of electronic excitations in molecules. In particular, coulomb plus exchange and correlation effects blueshift this independent particle transition about 2 eV in very good agreement with experiments (see Fig. 3). This is very important for the proper description of the ulterior excited state dynamics as the pump laser is tuned to resonance with this main excitation peak. Thus one may conclude that the static electronic properties of this complex are well described by the present approach.

Next the evolution of the Ba$\cdots$FCH$_3$ under high-field excitation was examined. The pump laser pulse applied had an energy of 2 eV, and power densities of 10^5 W/cm^2, 10^6 W/cm^2 and 5×10^6 W/cm^2 (these values are within the experimental range) and envelope formed by a linear ramp until the tenth optical cycle and then constant for the whole simulation. The polarisation was chosen randomly with respect to the Ba–F–C molecular axis. The dynamical simulations to be discussed below correspond to runs of a few picoseconds as this time scale turned out to be sufficient to get a qualitative picture of the laser induced fragmentation process. As the laser field populates the excited Born-Oppenheimer surfaces this scheme includes diabatic effects, while maintaining a good scaling with the size of the system. As we are interesting in addressing the competition between the two fragmentation channels (reactive one leading to BaF as fragment and non reactive leading to Ba* as fragment) and we treat the nuclei classically, for each random polarisation and laser intensity we have to monitor the ion trajectories over time corresponding to many different initial conditions (vibrational state of the molecule) in order to get some reliable statistics. With this approach we get only a qualitative picture of the process and to be more quantitative a quantum-mechanical description of the nuclear motion would be needed (which is beyond the scope of the present work and present computer facilities). However, as shown below, the calculations did provide insight into the physical mechanisms underlying the photoinduced fragmentation and channel selectivity. The probe laser with an energy pulse of 4.66 eV is applied at few time-delays, between 50 to 350 fs after the pump-laser. Electron ionisation is taking care by an imaginary absorbing potential at the box boundaries, this is important to qualitatively describe the proper physical process behind the photoinduced reaction. The simulations are stopped once one of the fragments had reached the boundary of our simulation box.

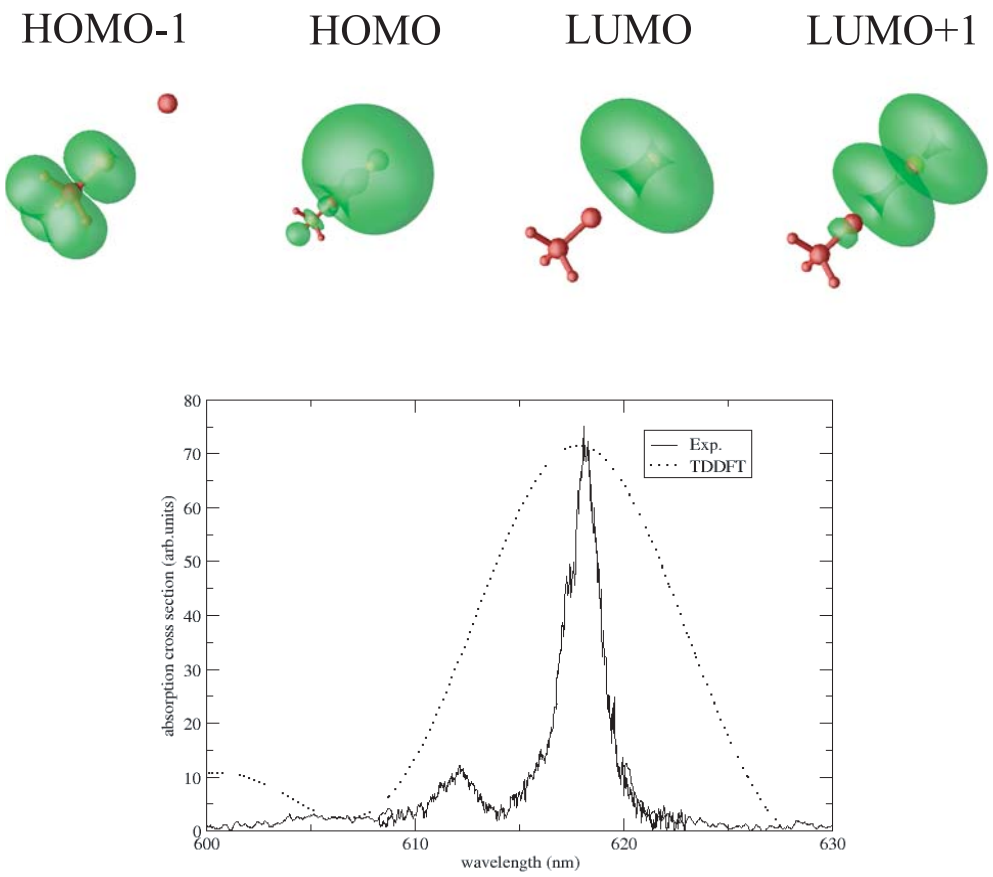

Fig. 3. Top: first two unoccupied (LUMO and LUMO+1) and two last occupied (HOMO and HOMO-1) orbitals of the $Ba\cdots FCH_3$ molecule. The HOMO-LUMO orbitals are mainly located at the Ba atom. It is clear that the orbitals are modified from being perfect atomic Ba (6*s* and 6*p*) orbital indicating that binding occurs through polarization effects and little charge overlap. This has important implications in the optical spectra (see text for details). Bottom: comparison between the computed and measured [12] optical absorption spectra (the calculated one has been scaled to match the strength of the experimental main peak). The strongest absorption peak can be assigned to the HOMO-LUMO transition. The agreement is very good taking into account the accuracy of the calculated spectrum (about 0.1 eV).

The theoretical simulation of the photodissociation process provides a clear picture of the cluster photodissociation mechanism, whose main features are the following: first the pump laser excited the HOMO-LUMO transition of molecule. This excitation is mainly localised at the Ba atom (see Fig. 3). Although this is the main excitation effect, the laser in the short time scale does also populate other Born-Oppenheimer surfaces that do play a role in the ensuing dynamics. Then, the coupling of this electronic excitation to the ions of the molecule brings the molecule to an excited vibrational state. The time scale for this coupling process in the simulation is of the order of 100–300 fs. During this vibration the laser continues to act and, eventually, leads to the detachment of the BaF fragment from the rest of the complex. If the probe laser is applied shortly after the pump laser, the excited state does not have time to decay into the excited-state molecular vibration, then as product we get the ionised $Ba\cdots FCH_3^+$ fragment. Only when the delay between pump and probe is above 100 fs we observe the appearance of the BaF^+ and Ba^+ fragments. It is important to emphasize that with only the pump laser and for all laser power densities, polarisation and initial configurations, we do not observe in the simulations any signal of the non-reactive channel (Ba fragment) and only the BaF fragment is obtained. This is in agreement with the fact that no Ba^+ ion signal was observed with the pump laser only, even though the higher fluences were employed. Thus, taking into consideration the energy of the process, one can conclude that the non-reactive photofragmentation channel here investigated, with the $\lambda = 266$ nm probing, corresponds to metastable $Ba(^1D_1, {}^3P)$ states.

The pump-probe simulations carried out showed the reactive BaF channel was always present, being the dominant and even the only one at high laser fluences. On the other hand, at small laser fluences, the non-reactive Ba^* channel appeared in the simulation in a few cases only. The time scale of theses two processes were found to be markedly different, whereas the reactive path occurs in few hundred fs, the non reactive part became active only at the picosecond regime and at low laser fluence regime To the best of our knowledge there is no experimental information about the reaction time associated to the non-reactive channel yielding Ba^* products. However,

the reaction time for the BaF channel has been measured to be about 270 fs by the femtosecond pump and probe technique [13,14]. Thus one can assume that the reaction time for the non-reactive channel could well be of the order of picoseconds as it is the (usual) case in photodissociation dynamics of van der Waals molecules. This distinct time dynamics of the two-photodissociation channels was clearly confirmed our TDDFT calculations.

The finding of a different time dynamics for the two cluster photodissociation channels does not justify by itself the observed laser fluence dependence of the branching ratio. It is also necessary a distinct laser fluence dependence for each individual photofragmentation channel. Interestingly, our simulation also showed that the higher the laser power the shorter the delay for the BaF production. In other words, the fast channel *accelerates* as the laser power is increased. Hence, to prevent this channel to full control the reaction path lower laser powers are needed in order to stay within the picosecond regime where the non-reactive Ba^* formation becomes active.

Simple kinematical arguments qualitatively support the distinct time dynamics of the two-photofragmentation channels found by our theoretical simulations. Indeed, for a given energy, E, the time required by the products to fly apart a critical distance d^* is given by $t^* = (\mu d^{*2}/2E)^{1/2}$ where μ is the product reduced mass. Thus, the two motions of the $Ba\cdots F\cdots CH_3^+$ transition state evolving into channel 1 ($BaF + CH_3$) or channel 2 ($Ba^{*}\cdot + F\cdots CH_3$), respectively, would need different times to reach the distance d^* after which one could consider that complete photodissociation has taken place. Actually, the kinematic branching would be $t_1^*/t_2^* = (\mu_1/\mu_2)^{1/2} = 1.41$. In other words, based on this crude kinematic model the reactive channel would be 1.41 times faster than the non-reactive one.

Now the question arises what could be the origin for the acceleration of the reactive BaF channel as the laser fluence increases? A rigorous answer to this crucial question would require a full quantum time dynamical study of the photofragmentation processes, which is out of the scope of the present letter. Nevertheless, some qualitative arguments can be given mainly based on the mechanism for the $Ba\cdots FCH_3 \rightarrow BaF + CH_3$ intracluster reaction. Certainly, based on the harpooning model reaction, which involves the electron transfer from the excited Ba to the F atom, an energy barrier should be expected for the reactive channel due to the negative electron affinity of the FCH_3 [27]. According to spectroscopic measurements from this laboratory [12] as well as from ab initio studies [26] the resonant excitation here used corresponds to the transition from the vibronic ground state X ($v'' = 0$) to the lowest vibrational level ($v' = 0$) of the excited A state of the $Ba\cdots FCH_3$. As a result, the necessary vibrational energy for the C–F stretch is not available and can only be obtained by internal conversion from the A state to the lower-lying excited electronic A' state. Thus, the energy transfer gained by this non-adiabatic coupling promotes the C–F stretch and, consequently, the electron transfer reaction. Strong support to this mechanism has been provided not only by ab initio calculations [26], but, especially, by pump and probe time-resolved photoelectron spectroscopy of both $Ba\cdots FCH_3^+$ and BaF^+ ions [28]. Thus the acceleration effect revealed by the theoretical calculation could perhaps be due to the lowering of the reaction barrier by the radiation field of the excitation laser. This type of effects has been shown in reaction dynamics calculations for elementary atom-diatom barrier reactions [29]. In this simple picture the higher the laser field the lower the barrier for the harpooning $Ba\cdots FCH_3 \rightarrow BaF + CH_3$ reaction and, consequently, the faster and more competitive the reactive channel with respect to the non-reactive one. Ultimately, at the high fluence limit, all the $Ba\cdots FCH_3$ photodissociation yield would be that of the reactive BaF product. Full quantum time dynamics calculations will be carry out to verify this working hypothesis.

The main finding of the present work is the distinct behaviour exhibited by the two-photodissociation channel yields, i.e. the reactive BaF and non-reactive Ba^* products, as the laser fluence of the excitation laser is increased. Such behaviour was attributed to (i) a different reaction time associated to each individual $Ba\cdots FCH_3$ photofragmentation channels and (ii) an "acceleration" effect of the faster channel as the laser power increased. The latter was attributed to a reduction of the energy barrier of the $Ba\cdots FCH_3 \rightarrow BaF + CH_3$ reaction induced by the coupling with the laser field. In this view, the higher the laser field the smaller the reaction barrier and the more competitive the BaF reactive channel. The combination of these two effects would then explain why the $(Ba^*)/(BaF)$ branching ratio changes from low to high laser fluences.

A key feature of the present investigation is the use of nanosecond laser pulses with the excitation laser fluence as the only adjustable parameter to change the outcome of the photoinitiated reaction. It has been shown [30] how the intensity of a femtosecond laser affects the dynamics of molecular vibrational wavepackets in several electronic states of Na_2, but it is, to our knowledge, the first time that it has been observed for a chemical reaction using nanosecond pump and probe pulses. An interesting conclusion of the present investigation is the possibility of laser control of multichannel reactions as long as the individual photofragmentation channels require a different time. In these cases the slow channel should first disappear by increasing the field of the pump laser recalling us that "*the slowest the channel the easiest to take*". Consequently, the different channels could be selectively closed by a continuous increase of the laser fluence. Undoubtedly, the simplicity of the proposed scheme makes it attractive for practical applications.

This work received financial support from MCyT of Spain Grants BQ2001-1461 and MAT2001-0946 and the Ramón Areces Foundation. AR and PME acknowledge support from the EC-RTN program NANOPHASE (contract HPRN-CT-2000-00167), Basque Country University and Basque Hezkuntza Saila. Calculations were performed on high-performance computing facilities of the DIPC and the

European Center for Parallelism of Barcelona (CEPBA). We wish to thank M.A.L. Marques and A. Castro for their continuous work on octopus as well as for useful discussions.

References

1. R.N. Zare, Science **279**, 1875 (1998)
2. S.R. Rice, Nature **409**, 422 (2000)
3. S. Shi, A. Woody, H. Rabitz, J. Chem. Phys. **88**, 6870 (1988)
4. M. Shapiro, P.J. Brumer, J. Chem. Phys. **84**, 4103 (1986)
5. M. Shapiro, P.J. Brumer, J. Chem. Phys. **97**, 6259 (1992)
6. L.-C. Zhu, V. Kleiman, X.-N. Li, S.P. Lu, K. Trentelman, R.J. Gordon, Science **70**, 77 (1995)
7. D. Tannor, S.A. Rice, J. Chem. Phys. **83**, 5013 (1985)
8. T. Baumert, M. Grosser, R. Thalweiser, G. Gerber, Phys. Rev. Lett. **67**, 3753 (1991)
9. A. Assion, T. Baumert, M. Bergt, T. Brixner, B. Kiefer, V. Seyfried, M. Strehle, G. Gerber, Science **282**, 919 (1998)
10. C. Daniel, J. Full, L. González, C. Lupulescu, J. Manz, A. Merli, S. Vajda, L. Woste, Science **299**, 536 (2003)
11. S. Skowronek, R. Pereira, A. González Ureña, J. Chem. Phys. **107**, 1668 (1997)
12. S. Skowronek, R. Pereira, A. González Ureña, J. Phys. Chem. **101**, 7468 (1997)
13. V. Stert, P. Farmanara, W. Radloff, F. Noack, S. Skowronek, J. Jimenez, A. González Ureña, Phys. Rev. A **59**, 1727 (1999)
14. P. Farmanara, V. Stert, W. Radloff, S. Skowronek, A. González Ureña, Chem. Phys. Lett. **304**, 127 (1999)
15. A. González Ureña, K. Gasmi, J. Jiménez, R.F. Lobo, Chem. Phys. Lett. **352**, 369 (2002)
16. E.K.U. Gross, F.J. Dobson, M. Petersilka, *Density Functional Theory* (Springer, New York, 1996)
17. G. Onida, L. Reining, A. Rubio, Rev. Mod. Phys. **74**, 601 (2002)
18. While the ionisation laser crosses the molecular beam perpendicularly, the excitation laser intersects the crossing point at an angle of about 5° with respect to the ionisation laser. Care was taken to achieve complete overlap of the two lasers in the intersection region by using two complementary double-diaphragms at the entrance and the exit window of the detection chamber. Thus, the pump laser beam overlaps totally the packet of complexes that is to be ionised by the probe laser
19. S. Skowronek, A. González Ureña, in *Atomic and Molecular beams: The state of the Art*, edited by R. Campargue (Springer, 2000), p. 353
20. S. Skowronek, A. González Ureña, Progr. React. Kin. Mech. **24**, 101 (1999)
21. The octopus project in aimed at describing by first-principles the electron-ion dynamics in finite and extended systems under the influence of arbitrary time-dependent electromagnetic fields. The program can be freely downloaded from `http//:www.tddft.org/programs/octopus`. For details see M.A.L. Marques, A. Castro, G.F. Bertsch, A. Rubio, Comp. Phys. Comm. **151**, 60 (2003)
22. A. Castro, M.A.L. Marques, J.A. Alonso, G.F. Bertsch, A. Rubio, Eur. J. Phys. B (in press, 2003)
23. This technique, first introduced in K. Yabana, G.F. Bertsch, Phys. Rev. B **54**, 4484 (1996) for the calculation of linear optical spectra of clusters, does not rely on perturbation theory, and is competitive with implementations in the frequency domain (A. Rubio, J.A. Alonso, X. Blase, L.C. Balbás, S.G. Louie, Phys. Rev. Lett. **77**, 247 (1996); E5442 (1996))
24. N. Troullier, J. Martins, Phys. Rev. B **43**, 1993 (1991). We used the core radii $r_c = 1.4$ and 1.29 a.u. for all the s, p pseudopotential components of C and F, respectively. For Ba we used a charged configuration including semicore states ($5s^2(r_c = 1.73)$ $5p^6(r_c = 2)$). Inclusion of scalar relativistic effects turn out to be crucial for the proper description of the excited state properties of the Ba atom
25. D.M. Ceperley, B.J. Alder, Phys. Rev. Lett. **45**, 1196 (1980); J.P. Perdew, A. Zunger, Phys. Rev. B **23**, 5048 (1981). For the qualitative picture we try to discuss in the present work the specific form of the exchange-correlation functional should not introduce major modifications (M.A.L. Marques, A. Castro, A. Rubio, J. Chem. Phys. **115**, 3006 (2001)). This is, however, untrue for studies of charge-transfer processes and isomerisation mechanisms
26. V. Stert, H.H. Ritze, P. Farnamara, W. Radloff, Phys. Chem. Chem. Phys. **3**, 3939 (2001)
27. P. Piecuch, J. Mol. Struct. **503**, 436 (1997)
28. V. Stert, P. Farnamara, H.H. Ritze, W. Radloff, K Gasmi, A. González Ureña, Chem. Phys. Lett. **337**, 299 (2000)
29. A.E. Orel, W.H. Miller, J. Chem. Phys. **70**, 4393 (1979)
30. T. Baumert, V. Engel, C. Meier, G. Gerber, Chem. Phys. Lett. **200**, 488 (1992)